J Electroceram (2008) 21:103–109
DOI 10.1007/s10832-007-9094-6

Gas-phase driven nano-machined TiO2 ceramics

Sehoon Yoo · Sheikh A. Akbar

Published online: 29 March 2007

Abstract A simple, inexpensive gas phase reaction termed as "nanocarving process" converts TiO_2 grains into arrays of single crystal nanofibers by selective and anisotropic etching. This process is conducted by exposing dense polycrystalline TiO_2 to a H_2/N_2 environment at 700 °C. The dimensions of nanofibers are around 20 nm in diameter and 1 μm in length. The preferred crystallographic orientation for the nanocarving process is the <001> direction. Nanoparticles composed of Fe and Ni were observed on the surface of TiO_2 that formed nanofiber tips. Sintering parameters before the nanocarving treatment play a critical role in the formation of nanofibers. As sintering temperature and time increased, the rate of nanofiber generation decreased. Moreover, it was observed that by varying the heat treatment conditions, it is possible to create other structures like nanowhiskers and nanofilaments. Nanowhiskers were formed by reoxidation of nanofiber-formed TiO_2 over 600 °C. Nano-filaments were generated by heat treating sintered TiO_2 in N_2-carrying water vapor at 700 °C.

Keywords TiO_2 · Nanocarving · Nanofibers · Nanorods · Nanowhiskers

1 Introduction

Nanostructured oxides have received significant attention in recent years due to their attractive electronic, photonic, catalytic, chemical, and bio-chemical properties. Titania (TiO_2) is an important engineering material that is widely used in chemical sensors [1], photocatalysts [2, 3], dye-sensitized solar cells [4], biosensors [5], biocompatible materials [6], and Li-based batteries [7]. Since the key chemical processes associated with such devices occur at TiO_2 surfaces, the surface morphology of the TiO_2 is an important device characteristic. Especially for gas sensing and photocatalytic applications, the high gas/solid interfacial areas associated with nanostructured oxide surfaces provide a significantly larger concentration of active sites, which, in turn, results in enhanced catalytic activity and chemical sensitivity [8].

Numerous approaches have been explored for tailoring the surface morphology of TiO_2 [9–11]. However, the widespread utilization of these processes is complicated by the conflicting demands for precise control of fine, well-ordered surface features and for low-cost, rapid mass production. Novel methods for fabricating well-organized oxide nanostructures that are simple and can be readily scaled up are needed to allow for large scale, cost-effective manufacturing.

Recently, we developed a novel, low-cost method for generating TiO_2 surfaces containing arrays of nanofibers. The process utilizes simple and highly scalable method involving gas phase reaction with non-combustible H_2/N_2 or H_2O. Therefore, it provides a) precise control of fine, well-ordered surface features and b) low-cost, rapid mass production. Unlike other nanostructure forming techniques, our technique doesn't require any sophisticated equipment. In this article, the synthesis of different nanostructures on TiO_2 by simple gas phase reactions are introduced and the properties of the nanostructures are discussed.

2 Experimental

The starting material was commercial anatase TiO_2 powder (Alfa Aesar, 99.9% pure) having an average particle size of

S. Yoo · S. A. Akbar (✉)
CISM, Department of Materials Science and Engineering,
Ohio State University, 291 Watts Hall, 2041 College Road,
Columbus, OH 43210, USA
e-mail: Akbar.1@osu.edu

32 nm. Batches of 0.3 g of TiO_2 powder were compacted into disks under a uniaxial pressure of 17.5 MPa in a stainless-steel die by single-end compaction. The disks were sintered at 1,200 °C for 6 h in ambient air except for the sample for a sintering time effect experiment, which was sintered at 1,300 °C for 3–12 h. After sintering, the phase changed from anatase to rutile and the sample sintered at 1,200 °C for 6 h had an average grain size of 2.74 μm which was measured by mean linear intercept method (ASTM standard). The sintered disks were 1 mm thick and 10 mm in diameter.

The sintered disks were, then exposed to a flowing atmosphere of 5% H_2/95% N_2 at 700 °C for 8 h by placing them in the middle of a furnace tube without any substrate. The end of the tube was sealed with O-rings and clamps and the oxygen partial pressure measured with an oxygen sensor (CG 1000, Ametek) was 3×10^{-22} atm. The absolute humidity measured with a humidity sensor (HMP234, Vaisala) was 0.2–0.5 g/m^3. The flow rate of H_2/N_2 gas was 500 ml/min. After H_2/N_2 heat treatment, the color of TiO_2 changed to bluish grey, which is generally observed for a reduced TiO_2 sample. Reoxidation of nanofiber-formed TiO_2 disks were conducted in the temperature range of 500–700 °C for 6 h in an ambient air atmosphere. For water vapor heat treatment, TiO_2 disks sintered at 1,200 °C for 6 h were heat treated in N_2-carrying water vapor. N_2 gas was passed through boiling water. Heating tapes were wrapped around tubing to avoid water condensation. For both the reoxidation and the H_2O heat treatment, the reactor setup was the same as the H_2/N_2 heat treatment except gas atmospheres.

A field emission gun scanning electron microscope (FEG-SEM, Model XL-30, Philips) was used to characterize the surface morphologies of the TiO_2 disk samples before and after exposure to the H_2 treatment. Before SEM observation, TiO_2 disk samples were coated with gold–palladium (Au–Pd) to prevent electron charging, which generally occurs in insulating materials. Average grain size was measured by the mean linear intercept method (ASTM standard). X-ray diffraction analyses (XRD, PAD-V diffractometer, Scintag) were used to evaluate the phase content of the disk surfaces before and after the reoxidation step. Cu Kα radiation was used for the XRD. X-ray photoelectron spectroscopy (XPS, Perkin–Elmer Model 550 ESCA/Auger Spectrometer) was used to determine the oxidation state of titanium before and after the H_2/N_2 treatment. For the XPS analysis, H_2/N_2 heat treated TiO_2 samples were kept in the tube under 5% H_2/N_2 gas after heat treatment. The XPS spectra were obtained at room temperature by using Mg Kα radiation and the pressure of the spectrometer chamber was 10^{-9} torr. For comparison of peak positions for different samples, the C 1s peak position was used to correct for binding energy shifts between samples.

3 Results and discussion

Figure 1 shows scanning electron microscope (SEM) image of the surface of a TiO_2 sample before and after the nanocarving. As can be seen, TiO_2 grains converted into aligned nanofibers, which had a diameter of around 20 nm and lengths of 1 μm. Before nanocarving [Fig. 1(a)], polycrystalline TiO_2 disk samples were prepared by sintering powder compact at 1,200 °C for 6 h. The nanofibers were only formed on the surface and the depth of nanofiber formed region ranged from 0.7 to 1 μm. The phase of nanofibers was determined to be rutile TiO_2 by XRD, TEM [12] and XPS [13], although the nanofibers were generated under a reducing environment of H_2/N_2. Based on a time sequence SEM experiment [12] of a specific grain, it was determined that the nanofiber formation was by an etching process and not by a growth process. In addition, thermogravimetric analysis (TGA) [14] showed that the weight of TiO_2 decreased during H_2/N_2 treatment, which confirmed that the nanofiber formation was due to an etching process. The etching direction was determined to be

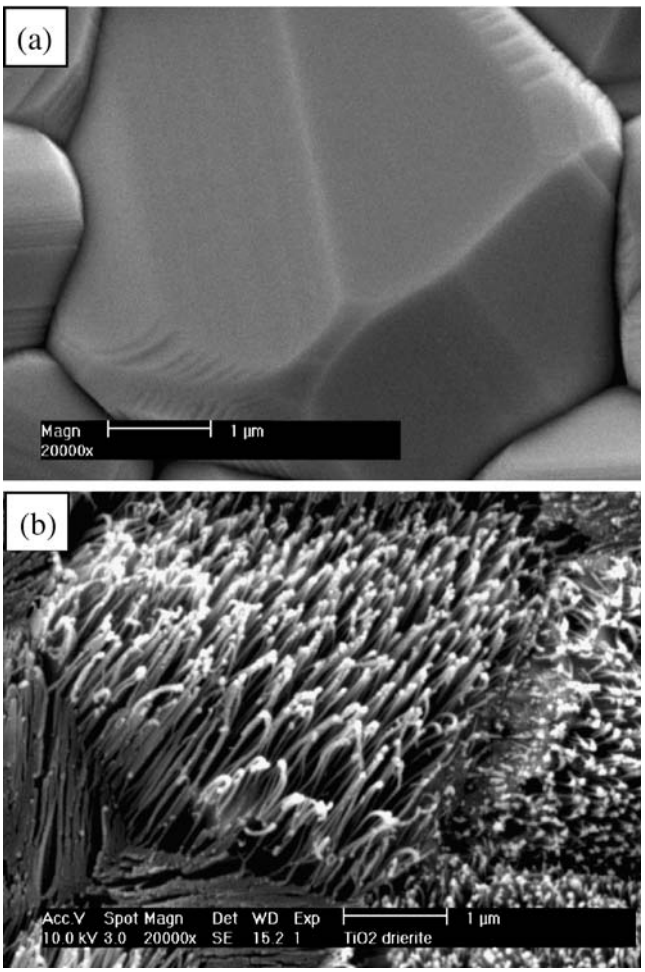

Fig. 1 Scanning electron microscope (SEM) images of TiO_2 surface (**a**) before and (**b**) after nanocarving

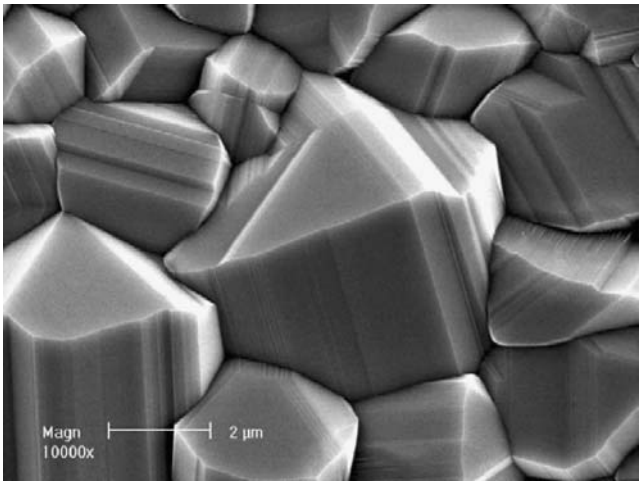

Fig. 2 SEM micrograph of a TiO_2 disk surface after 100% N_2 treatment at 700 °C for 8 h

<001> from TEM observation [12]. This selective and anisotropic etching process was dubbed "Nanocarving."

Nanocarving was achieved in a mixed hydrogen/nitrogen gas atmosphere. To determine the role of nitrogen gas, if any, TiO_2 specimen were heat-treated in 100% N_2 atmosphere under similar conditions as the H_2/N_2 nanocarving process (700 °C, 8 h). Figure 2 shows SEM micrographs of the surface of TiO_2 after 100% N_2 treatment, which shows no evidence of etching or nanofiber formation. To confirm that only H_2 gas plays a role on the nanocarving process, N_2 was switched with another inert gas, Ar (Fig. 3). In 5% H_2/ 95% Ar atmosphere, nanofibers were observed on the surface indicating that only hydrogen is the reacting gas species.

Figure 4 shows that nanofibers formed on TiO_2 grains. In Fig. 4(a), only half of the grain transformed into nanofibers and the region where no fiber was generated had nanoparticles with the diameter of few tenths of nanometers. In addition, the end tips of nanofibers were round and possessed similar diameters as the nanoparticles, i.e. the nanoparticles appeared to be sitting on the end tips of nanofibers. Previous TEM and EDS results showed that the nanoparticles were enriched in Fe and Ni [12]. In addition, the nanoparticles were likely to be metallic alloys since the O peak was not observed in the EDS pattern [12]. These nanoparticles appear to have been generated during the H_2/N_2 gas treatment by the external reduction of the Fe and Ni oxides present as impurities in the starting TiO_2 powder.

The segregation of impurities such as Fe, Al, Nb, and Ca in TiO_2 has been reported in many studies [15–18]. Gazzoli et al. [19] studied H_2 reduced Fe-doped (up to 8%) TiO_2 and found that Fe (III) ions were reduced by a two step process (Fe(III) → Fe (II) → Fe (0)). The metallic Fe (0) segregated in the temperature range of 770–1,070 K. They also found significant weight loss of Fe doped TiO_2 during H_2 reduction, while pure TiO_2 did not show much weight loss below 1,070 K. The weight change resulted from both reduction of iron oxide and titanium oxide and the weight loss of TiO_2 was 30% of the total weight loss in the case of 0.3% Fe doped TiO_2. They proposed that near the segregated Fe particles in contact with TiO_2, a strong metal-semiconductor interaction (SMSI) occurred, causing a reduction of the nearby TiO_2 matrix. SMSI is generally believed to occur for group VIII elements (Fe, Co, Ni, Ru, Rh, Pd, Os, Ir, and Pt) on TiO_2. Rekoske and Barteau [20] measured the weight change of TiO_2 powder mixed with one of the VIII elements, Ru, during H_2 heat treatment. They observed that the rate of mass loss during H_2 heat treatment was higher for Ru/TiO_2 than that for pure TiO_2. Chen and White [21] observed the reduction of Pt/TiO_2 by measuring electron spin resonance (ESR) signal associated with Ti^{3+} cations at 200°C. At the same temperature, they didn't observe any reduction of pure TiO_2. This finding was supported by temperature programmed reduction studies which indicate that TiO_2 reduction becomes measurable at lower temperatures when Pt is present on TiO_2 [22, 23]. In our system, the segregated Fe or Ni particles may act as catalysts to enhance the reduction of TiO_2 near the segregated particles. Hence, the selective etching for nanofiber formation may be caused by the weight loss near the segregated particles.

The controllable factors for the optimization of the nanocarving are the sintering condition (temperature and time) and H_2/N_2 heat treatment condition (temperature and flow rate). The degree of nanofiber formation was dependent on the sintering temperature and time. From the sintering temperature variation [13], it was clearly observed that the rate of nanofiber formation decreased as the sintering time and temperature increased. Sintering time also affected the rate of the nanocarving process. To understand the sintering time effect, TiO_2 disks were sintered at 1,300 °C for 3 and

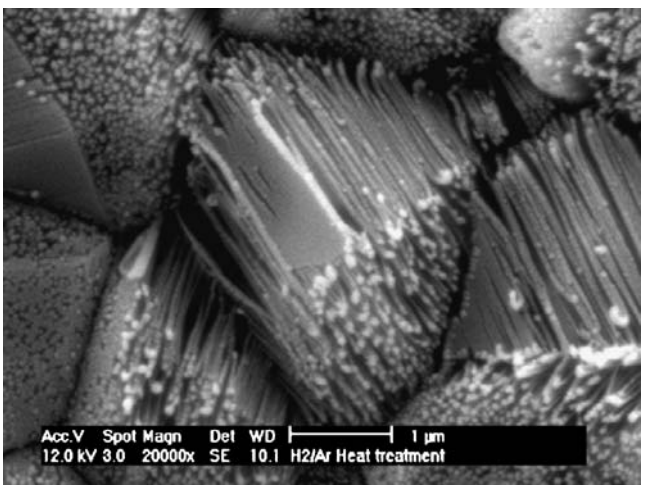

Fig. 3 SEM micrograph of a TiO_2 disk surface after 5% H_2/95% Ar treatment at 700 °C for 8 h

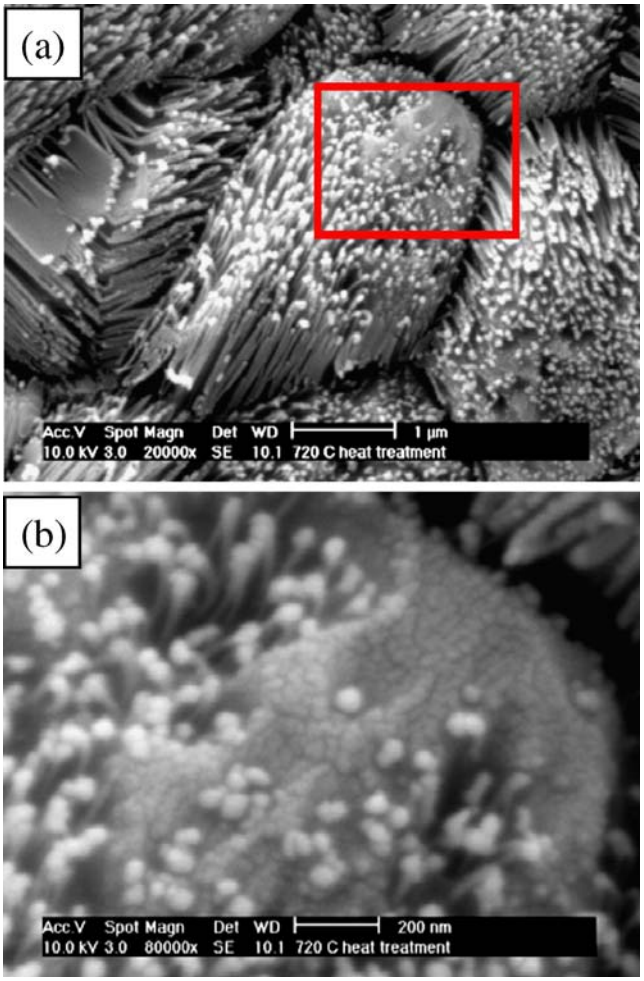

Fig. 4 SEM micrographs of a TiO_2 disk surface after H_2/N_2 heat treatment, showing nanofibers with nanoparticles; (**a**) low magnification and (**b**) high magnification of the area enclosed by a square in (**a**)

12 h and then were processed under the same condition (700 °C for 8 h in 5% H_2/N_2 atmosphere). Figure 5 shows SEM micrographs of two different TiO_2 samples after the nanocarving process. The 3 h heat-treated sample showed well-developed nanofibers after the H_2/N_2 treatment [Fig. 5(a)]. However, 12 h heat-treated sample didn't show well-developed nanofibers, even though some etching was observed on the surface [Fig. 5(b)].

From the sintering condition variations, it was clearly observed that the rate of nanofiber formation decreased as the sintering time and temperature increased. Since the etching process is caused by H_2 reaction with TiO_2, the rate of nanofiber formation should be dependent on the reaction rate. Khader et al. [24] proposed four steps of H_2 reaction with TiO_2: 1) adsorption of H_2 on the TiO_2 surface, 2) reaction of adsorbed hydrogen with lattice oxygen to form water, 3) water vapor desorption, and 4) diffusion of bulk oxygen to the surface to fill the removed oxygen sites. They also proposed that the rate of H_2 adsorption controlled the overall rate of H_2 reduction of TiO_2 initially, while the rate of oxygen anion diffusion became rate controlling at longer times. From their data, the transition from adsorption to diffusion control process took about 40 min for 500 °C of H_2 reduction, and the extrapolated value of the transition time at 700 °C was 8 min. Therefore, most of the time during the 8 h/700 °C nanocarving process of TiO_2, the rate of nanofiber formation would be controlled by the diffusion process.

The proposed oxygen anion diffusion during H_2 reduction of TiO_2, however, conflicts with results showing that Ti cation diffusion is orders of magnitude faster than that of O anion diffusion [25, 26]. This supports diffusion of Ti cations from the surface to the bulk during the H_2 reaction with TiO_2.

Since an increase in the sintering temperature and time cause an increase in the grain size of TiO_2 (and a decrease in grain boundary density) and since Ti cation diffusion is generally dependent on the grain boundary density, the sintering condition variation is likely to change the Ti diffusion rate, and thereby the rate of nanofiber formation.

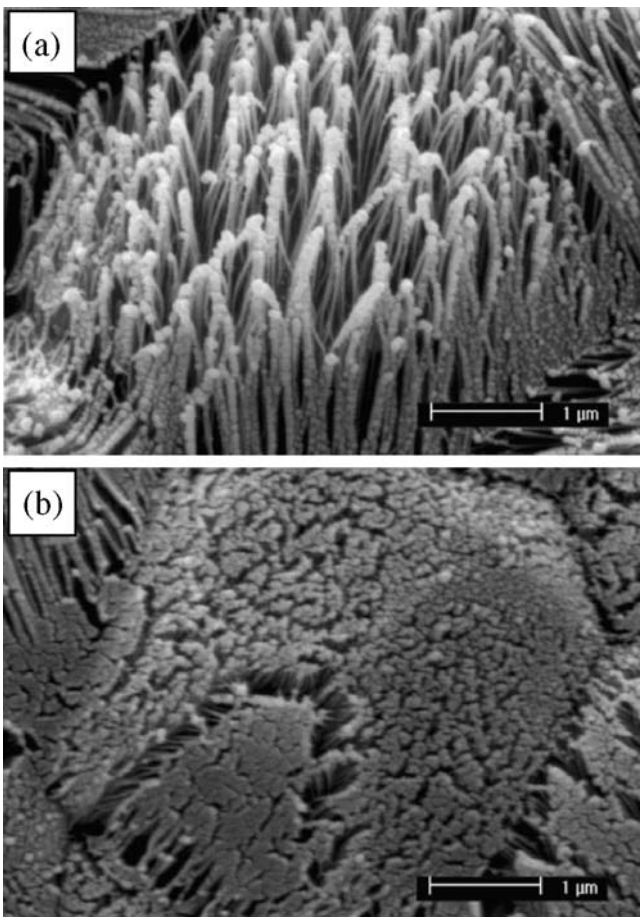

Fig. 5 SEM micrographs of TiO_2 sintered for different times at 1,300 °C and then heat-treated at 700 °C for 8 h in H_2 atmosphere. The sintering times were: (**a**) 3 h and (**b**) 12 h

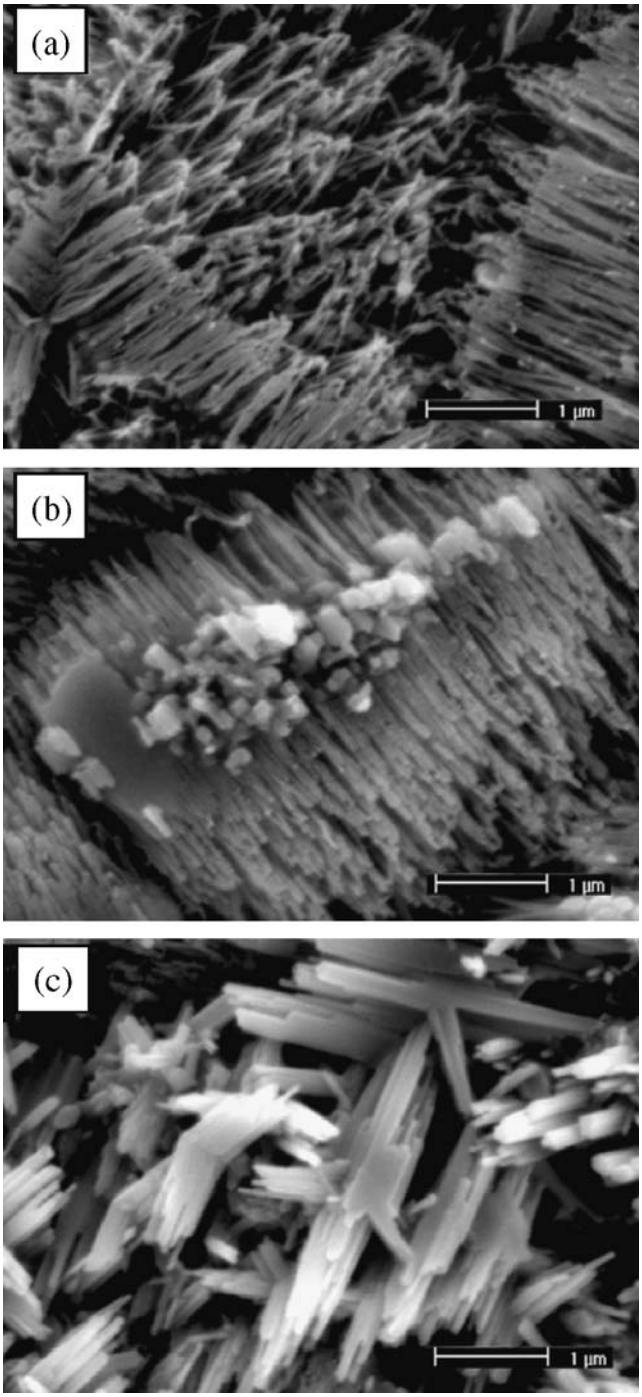

Fig. 6 SEM images of a TiO_2 disk surface after reoxidation of TiO_2 nanofibers. The nanofibers were annealed in air atmosphere at (**a**) 500 °C, (**b**) 600 °C, and (**c**) 700 °C

As expected, the average grain size of TiO_2 increased from 1.57 to 7.70 μm as sintering temperature and time increased. The average grain sizes of the samples showing well-developed nanofibers are 1.57 μm (1,100 °C, 6 h), 2.54 μm (1,200 °C, 6 h) and 3.78 μm (1,300 °C, 3 h). Above 4 μm of average grain size, the nanofibers were not well-developed during H_2 heat treatment. The effective diffusivity from lattice and grain boundary diffusion can be represented by the following equation [27],

$$D_{eff} = D_l + \frac{\delta}{G}\left(D_{gb} - D_l\right) \quad (1)$$

where, D_l and D_{gb} are lattice and grain boundary diffusivity, respectively, and G and δ are width of grain (grain size) and grain boundary, respectively. The effective diffusivity is dependent on 1/(grain size) from the above equation if the other variables do not change much. Therefore, as the grain size increased by sintering, the diffusivity of Ti cation is likely to have decreased, which may have caused the reduction of the etching rate for nanofiber formation.

Preliminary gas sensing tests using these structures show promise [14, 28]. For sensing in combustion environments, the nanofibers would be exposed to ambient atmosphere at elevated temperatures, which may cause microstructural changes in TiO_2. To study microstructural changes in ambient atmosphere at an elevated temperature, the nanofiber-formed TiO_2 was reoxidized in the temperature range of 500–700 °C for 8 h in air. Figure 6 shows microstructural evolution of TiO_2 nanofibers after the air annealing. Below 500 °C annealing, nanofibers retained the structure. As the temperature of air annealing increased to 600 °C, particles of 100–200 nm size began to form on the nanofiber formed TiO_2 grains. As the reoxidation temperature increased, the particles shown at 600 °C were seen to grow to form nanowhiskers. The phase of reoxidized TiO_2 (at 700 °C for 8 h) surface was found to be rutile TiO_2 based on XRD.

To date, no study about the massive growth of nanowhiskers by reoxidation has been reported. However, reoxidation studies at the atomic scale, with surface analysis tools like scanning tunneling microscopy (STM), have been reported [29]. Onishi et al. [30] proposed Ti^{n+} interstitial

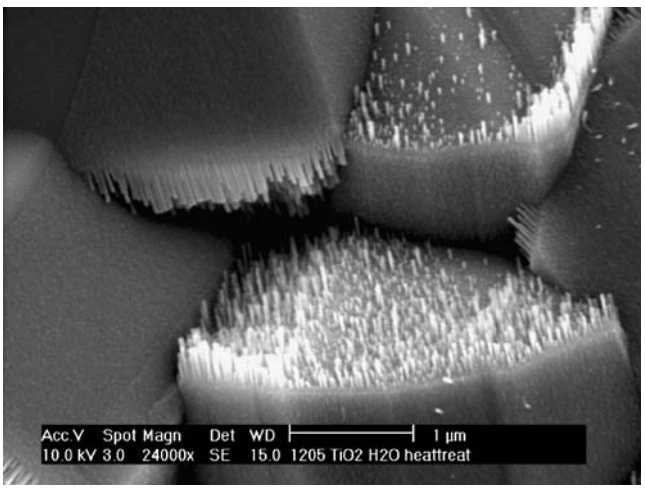

Fig. 7 SEM micrographs of TiO_2 surface after N_2 carrying H_2O heat treatment (at 700 °C for 8 h). Before the H_2O heat treatment, the TiO_2 was sintered at 1,200 °C for 6 h in air atmosphere

diffusion to the surface during the reoxidation of reduced TiO_2. Li et al. [31] observed the formation of pseudo-hexagonal rosettes (6.5 Å×6 Å) and small [110]-oriented islands, along with [001]-oriented strands, at temperatures from 470 to 660 K. Smith et al. [32] observed the surface of TiO_2 (110) single crystal with scanning tunneling microscopy (STM) during reoxidation of the vacuum or Ar ion reduced TiO_2 between 573 and 1,000 K at pressures from 5×10^{-11} to 2×10^{-9} atm O_2. From STM observation, they reported the growth of TiO_2 via the combination of O_2 with mobile Ti^{3+} ions. Recent work by Henderson [33] provides good evidence for titanium interstitial diffusion mechanism in rutile TiO_2. He also proposed that the bulk TiO_2 acts as a sink for excess surface Ti generated from the reduction of TiO_2. Therefore, Ti^{3+} ions are cycling between the bulk and the surface by reduction or reoxidation, respectively.

Gas phase reaction with H_2O creates another novel nanostructure on the TiO_2 surface. Very tiny nanofilaments with diameters of around 10 nm were developed with heat-treatment in N_2 carrying water vapor atmosphere (Fig. 7). TiO_2 disks were prepared by sintering at 1,200 °C for 6 h and then H_2O heat treatment was performed at 700 °C for 8 h. The dimension of the nanofibers formed in water vapor atmosphere was much smaller than that of the nanofiber formed by H_2/N_2 treatment. In the low magnification image (Fig. 7), the nanofibers were observed to be formed only on a specific face of each grain. When the grain was compared with the equilibrium crystal shape of rutile TiO_2 [34], the specific face on which nanofibers were formed appeared to be (001) plane of rutile TiO_2. In addition, the fibers by H_2O heat treatment appeared to be formed by growth rather than etching.

The exact reason why nanofibers formed with H_2O heat treatment is still not clear. However, the apparent nanofiber growth on the (001) plane may be due to adsorbed hydroxyl groups reacting with small impurities or titanium interstitials, which diffuse along the <001> direction [35]. Several researchers have shown that interstitial Ti^{3+} cations readily diffuse along <001> channels of the bulk rutile structure and hop in the $\langle 1\,\bar{1}\,0\rangle$ direction between <001> channels [36, 37]. In the future, systematic studies are required to understand the composition and structure of the nanofilaments generated by H_2O treatment.

4 Conclusions

Simple gas phase reaction under different conditions creates various nanostructures of TiO_2. TiO_2 nanofibers are produced by a nanocarving process (heat treatment in H_2/N_2 700 °C for 8 h), which is a selective and anisotropic etching technique. The nanofibers form only on the surface and the dimensions are around 20 nm in diameter and 1 μm in length. The phase of nanofibers is confirmed to be rutile TiO_2 and the direction is <001>. The rate of nanocarving increases as the sintering temperature and time decrease indicating a grain-boundary dominated diffusion process. Nanowhiskers are grown on nanofiber formed surface by reoxidation at 700 °C for 8 h in air. Nanofilaments are grown on the TiO_2 surface by H_2O heat treatment at 700 °C for 8 h.

Acknowledgements This work was supported by the U.S. National Science Foundation grant, DMR-0309558.

References

1. L.D. Birkefeld, A.M. Azad, S.A. Akbar, J. Am. Ceram. Soc. **75**, 2964 (1992)
2. S. Matsuda, A. Kato, Appl. Catal. **8**, 149 (1983)
3. Y. Nakato, H. Akanuma, J. Shimizu, Y. Magari, J. Electroanal. Chem. **396**, 35 (1995)
4. B. O'Regan, M. Graetzel, Nature **353**, 737 (1991)
5. E. Topoglidis, A.E.G. Cass, G. Gilardi, S. Sadeghi, N. Beaumont, J.R. Durrant, Anal. Chem. **70**, 5111 (1998)
6. Q. Li, G. Luo, J. Feng, Electroanalysis **13**, 359 (2001)
7. C. Natarajan, K. Setoguchi, G. Nogami, Electrochim. Acta 43, 3371 (1998)
8. G. Li, X. Zhang, S. Kawi, Sens. Actuators, B **60**, 64 (1999)
9. Z. Miao, D. Xu, J. Ouyang, G. Guo, X. Zhao, Y. Tang, Nano Lett. **2**, 717 (2002)
10. S.K. Pradhan, P.J. Reucroft, F. Yang, A. Dozier, J. Cryst. Growth **256**, 83 (2003)
11. X.Y. Zhang, L.D. Zhang, W. Chen, G.W. Meng, M.J. Zheng, L.X. Zhao, F. Phillipp. Chem. Mater. **13**, 2511 (2001)
12. S. Yoo, S.A. Akbar, K.H. Sandhage, Adv. Mater. **16**, 260 (2004)
13. S. Yoo, S.A. Akbar, K.H. Sandhage, Ceram. Int. **30**, 1121 (2004)
14. S. Yoo, Ph.D. Thesis, The Ohio State University (2005)
15. F.J. Berry, C. Xu, S. Jobson, R. Strange, J. Chem. Soc., Faraday Trans. 1(85), 3891 (1989)
16. R. Bouchet, A. Weibel, P. Knauth, G. Mountjoy, A.V. Chadwick, Chem. Mater. **15**, 4996 (2003)
17. F. Gracia, J.P. Holgado, F. Yubero, A.R. Gonzalez-Elipe, Surf. Coat. Technol. **158–159**, 552 (2002)
18. C.D. Terwilliger, Y.-M. Chiang, Acta Metall. Mater. **43**, 319 (1995)
19. D. Gazzoli, G. Minelli, M. Valigi, Mater. Chem. Phys. **21**, 93 (1989)
20. J.E. Rekoske, M.A. Barteau, J. Phys. Chem. B **101**, 1113 (1997)
21. B.H. Chen, J.M. White, J. Phys. Chem. **87**, 1327 (1983)
22. T. Huizinga, J. Van Grondelle, R. Prins, Appl. Catal. **10**, 199 (1984)
23. P.G. Menon, G.F. Froment, Appl. Catal. **1**, 31 (1981)
24. M.M. Khader, F.M.N. Kheiri, B.E. El-Anadouli, B.G. Ateya, J. Phys. Chem. **97**, 6074 (1993)
25. J.R. Akse, H.B. Whitehurst, J. Phys. Chem. Solids. **39**, 457 (1978)
26. K. Hoshino, N.L. Peterson, C.L. Wiley, J. Phys. Chem. Solids. **46**, 1397 (1985)
27. P. Shewmon, *Diffusion in Solids.* (TMS, Warrendale, PA, 1989)
28. C. Carney, S. Yoo, S.A. Akbar, Sens Actuators, B **108**, 29 (2005)
29. P. Stone, R.A. Bennett, M. Bowker, New J. Phys. [Electronic Publication] 1, Article 8 (1999)
30. H. Onishi, Y. Iwasawa, Surf. Sci. **313**, L783 (1994)

31. M. Li, W. Hebenstreit, L. Gross, U. Diebold, M.A. Henderson, D. R. Jennison, P.A. Schultz, M.P. Sears, Surf. Sci. **437**, 173 (1999)
32. R.D. Smith, R.A. Bennett, M. Bowker, Phys. Rev., B **66**, 035401 (2002)
33. M.A. Henderson, Surf. Sci. **419**, 174 (1999)
34. I. Kostov, *Mineralogy.* (Oliver and Boyd, Edinburgh, London, 1968)
35. J. Sasaki, N.L. Peterson, K. Hoshino, J. Phys. Chem. Solids. **46**, 1267 (1985)
36. N.L. Peterson, J. Sasaki, NATO ASI Ser., Ser. B: Physics **129**, 269 (1985)
37. K. Ruebenbauer, U.D. Wdowik, M. Kwater, Phys. Rev., B. **54**, 4006 (1996)